agriculture

MDPI

Article

How Microplastics Influence the Microbial Communities of Periphytic Biofilm Between the Paddy Soil and Water Interface: A Microcosm Study

Yufei Dong [1,2], Congying Han [1,2], Shuai Pan [1,2], Xinli Lin [1,2], Lingyuan Chen [1,2], Yinlong Zhang [1,2] and Haiying Lu [1,2,*]

[1] Co-Innovation Center for the Sustainable Forestry in Southern China, College of Ecology and Environment, Nanjing Forestry University, Nanjing 210037, China
[2] National Positioning Observation Station of Hung-Tse Lake Wetland Ecosystem in Jiangsu Province, Hongze 223100, China
* Correspondence: luhaiying@njfu.edu.cn

Abstract

Microplastics (MPs) are emerging pollutants that affect soil–microbe interactions in paddy ecosystems. Periphytic biofilms (PBs) are complex microbial consortia that ubiquitously distribute at the soil–water interface of paddy ecosystems, playing essential roles in nutrient cycling and pollutant migration. However, whether MPs affect the community composition of PBs remains largely unknown. This microcosm study investigated the effects of three types of MPs (polyacrylonitrile, PAN; polyethylene, PE; and polyethylene terephthalate, PET) on the community characteristics of PBs via high-throughput sequencing (16S/18S rRNA) technology. Results showed that the addition of all MPs significantly increased the biomass and chlorophyll-a content of PBs, with PAN inducing the maximum increase (by 331.9% and 128.6%). However, all MPs had no significant effect on the PB α-diversity of bacterial and eukaryotic communities ($p > 0.05$). As for PB composition, PAN and PET increased the relative abundance of Cyanobacteria, Proteobacteria and Holozoa, PE increased that of Cyanobacteria, Bacteroidota and Blastocladiomycota, and all MPs decreased the relative abundance of *Chloroflexi*, *Actinobacteriota* and *Basidiomycota*. Furthermore, PET decreased the predicted functional potential of natural polymer degradation (*cellulolysis*, *ligninolysis*, *xylanolysis*, *ureolysis*), nitrogen fixation and nitrate ammonification, while PE increased predicted potential for plastic degradation, nitrate reduction and denitrification. Co-occurrence network analysis suggested that the PE network showed higher connectivity and lower modularity, while the PAN network showed higher modularity. This study advances our understanding of soil MPs–microbe interactions under high-concentration conditions. It also suggests that PB community characteristics may serve as potential bioindicators for soil MP pollution.

Keywords: microplastics; periphytic biofilms; microbial community; functional prediction; high-throughput sequencing

Check for updates

Academic Editor: Dharmappa Hagare

Received: 27 March 2026
Revised: 20 April 2026
Accepted: 22 April 2026
Published: 28 April 2026

Copyright: © 2026 by the authors. Licensee MDPI, Basel, Switzerland. This article is an open access article distributed under the terms and conditions of the Creative Commons Attribution (CC BY) license.

1. Introduction

Microplastics (MPs), defined as synthetic polymer particles smaller than 5 mm, have emerged as a pervasive and persistent environmental contaminant of global concern [1]. Quantitative surveys confirm widespread MP contamination in paddy fields: Southern China averages 4176 ± 2976 items/kg (32 polymer types, dominated by PET 28.8% and

PVC 13.5%) [2]; Shanghai rice paddies are in the range of 233–1733 particles/kg (PP/PE 24.30%, PS 21.40%) [3]. Agricultural soils, particularly those in rice paddy ecosystems, are recognized as major sinks for MPs, receiving inputs from plastic mulches, sewage sludge, atmospheric deposition, and irrigation water [4,5]. Once in the soil, MPs can alter physical properties (such as porosity and water retention), introduce chemical additives, and adsorb existing pollutants, thereby imposing multifaceted stress on soil biota and potentially disrupting essential ecosystem functions mediated by microorganisms [6,7]. In paddy ecosystems, MP contamination alters soil's physical, chemical, and biological properties [8]. MPs often coexist with heavy metals (HMs), adsorbing them via electrostatic attraction, and surface complexation, with adsorption capacity depending on MP type, aging degree, and environmental factors [9]. The effects of MPs on soil microbial populations have been shown in an increasing amount of research. The shape, variety, and enzyme activity of bacterial and fungal communities can be dramatically changed by both conventional (like polyethylene, PE; polystyrene, PS) and biodegradable (like polylactic acid, PLA) MPs [10,11]. These effects are often polymer-specific. For instance, biodegradable MPs may release bioavailable carbon, triggering catabolite repression and shifting community metabolic pathways, whereas conventional MPs might selectively enrich taxa involved in specific biogeochemical cycles like nitrification [12].

However, most MPs research has focused on microbes in bulk soil, with little attention paid to periphytic biofilms (PBs), the microbial aggregates at the soil–water interface. In paddy ecosystems, PBs are complex, matrix-enclosed microbial consortia colonizing submerged surfaces, comprising photoautotrophs (algae, cyanobacteria), heterotrophic bacteria, fungi, and protozoa embedded in extracellular polymeric substances (EPSs) [13]. PBs are fundamental to ecosystem productivity, nutrient cycling, pollutant removal, and food web dynamics [14–16]. Due to their sensitivity to environmental change, PB communities serve as excellent "biological sentinels" for monitoring ecosystem health [17]. The input of MPs into paddy environments presents a novel perturbation to PBs. MPs can act as artificial substrates for colonization (forming the "plastisphere"), alter local microenvironments, leach chemicals, and potentially compete with natural substrates, thereby reshaping PBs' community structure and function [18,19]. MPs have polymer-specific effects on soil microbes: PLA can reduce bacterial diversity and enrich genera such as *Nocardioides*, *Arthrobacter*, and *Ramlibacter*, which are known for degrading complex compounds, while Polyvinyl Chloride (PVC) causes only temporary shifts [20]; low concentrations (0.1–1%) of PE alter bacterial abundance, enzyme activities, and nutrient cycling [10,11].

Previous MPs–microbe studies have focused on bulk soil communities, overlooking periphytic biofilms (PBs) at the soil–water interface. How different MP polymer types shape PB community structure, functional potential, and co-occurrence networks under controlled conditions remains uncompared. To address this gap, we selected three MPs with distinct environmental relevance and surface chemistries: PAN (hydrophilic, from agricultural textiles), PE (hydrophobic, dominant in Chinese farmlands), and PET (moderately hydrophilic, abundant in paddy soils) [2,8,10,11].

We therefore hypothesized that MP addition significantly alters the microbial community composition and functional potential of PBs. To test this hypothesis, we investigated the effects of three types of MPs (PAN, PE, PET) on the growth and microbial community structure of PBs at the paddy soil–water interface. We integrated measurements of biomass and chlorophyll-a, high-throughput sequencing of 16S and 18S rRNA genes, functional prediction (FAPROTAX, FUNGuild), and co-occurrence network analysis. The objectives of this study were to: (1) investigate the effects of MP addition on the growth of PBs; (2) evaluate the impacts of MPs on the microbial community composition of PBs; and (3) predict how MPs alter the metabolic functions of PBs. This study provides the first comparative

assessment of how three distinct MP types (PAN, PE, PET) affect PB growth, microbial community composition, predicted functional potential, and co-occurrence network structure at the paddy soil–water interface under microcosm conditions.

2. Materials and Methods

2.1. Study Site and Sampling

To investigate the effects of MPs on the development and function of PBs in paddy systems, a microcosm experiment was conducted. About 10 kg of surface soil (0–20 cm) was collected in 2023 from a paddy field at the Jiangsu Academy of Agricultural Sciences (N 32°2′1.17″, E 118°52′31.84″). The soil was air-dried at room temperature, and visible debris such as stones, agricultural plastic films, and plant residues were manually removed. The paddy soil used had the following basic physicochemical properties: pH of 7.7 (soil:water = 1:2.5, *w*/*v*), total nitrogen (TN) of 1.1 g/kg, total phosphorus (TP) of 0.9 g/kg, total potassium (TK) of 16.2 g/kg and total organic carbon (TOC) of 9.7 g/kg, determined according to standard soil analytical methods [21]. The soil was then homogenized and passed through a 2 mm sieve for subsequent use.

Natural PBs were collected from the same paddy field site, homogenized in sterile water, and pre-cultured in BG11 medium ($NaNO_3$ 1500 mg/L, K_2HPO_4 40 mg/L, Na_2CO_3 20 mg/L, $MgSO_4{\cdot}7H_2O$ 75 mg/L, $CaCl_2{\cdot}2H_2O$ 36 mg/L, citric acid and ferric ammonium citrate 6 mg/L, EDTA-Na_2 1 mg/L) for 7 days under controlled conditions (12 h light at 30 °C, 65% relative humidity, and 3000 Lx; 12 h dark at 25 °C, 65% relative humidity, and 0 Lx) to obtain a uniform inoculum. A static shallow water layer (approximately 2 cm depth) was maintained without forced aeration. The pre-cultured and amplified PB suspension (PB:water = 1:10) was evenly inoculated onto the soil surface of each Petri dish. The microcosms were maintained for 30 days under the same diurnal conditions. After the 30-day incubation, the developed PBs were carefully collected from the soil surface for subsequent determination of biomass, chlorophyll-a and high-throughput microbial sequencing.

2.2. Microcosm Setup

Three common agricultural MPs were selected in this study: PAN, extensively applied in agricultural textiles (e.g., fishing nets and ropes) and prone to accumulation in aquatic water bodies and sediments; PE, the primary constituent of agricultural plastic films and a common farmland contaminant; and PET, commonly used in synthetic fibers and characterized by high chemical stability and resistance to microbial degradation. The MPs were irregular granules with a nominal size of 200 μm. The actual particle size was 200 ± 10 μm (mean ± range). Purity was 99% for all three polymers, with no additives or plasticizers (pure resin).

The experiment was carried out in July 2023. For each treatment, 400 g of this soil was thoroughly homogenized with MPs at a concentration of 0.5% (*w*/*w*), corresponding to 2 g of MPs per 400 g of soil. This concentration is higher than typical field levels. Field soils usually contain less than 0.1% (*w*/*w*) MPs [2,3]. However, many soil microplastic microcosm studies use concentrations between 0.1% and 5% (*w*/*w*) [22,23]. These higher concentrations help to amplify detectable effects. Each treatment (CKU, PAN, PE, PET) was performed with three independent biological replicates (n = 3, total 12 microcosms), giving a total of 12 microcosm units. The soil–MPs mixture was then transferred into square Petri dishes (12 cm × 12 cm).

2.3. Determination of PB Biomass and Chlorophyll-a Content

The biomass of PBs was determined via the gravimetric method based on dry weight. All biomass and chlorophyll-a measurements were performed on three independent biological replicates per treatment (n = 3). After collection, the wet weight of each biofilm sample was recorded immediately. Adherent soil particles on the samples were then rinsed thoroughly, and the samples were freeze-dried to a constant weight. The dry weight (DW) of PBs was defined as the weight of the freeze-dried samples, with biomass yield expressed as mg dry weight per gram of initial soil (mg/g) or per unit area (g/cm) according to the experimental design. Chlorophyll-a content in PBs was determined by spectrophotometry. Freeze-dried samples (20–50 mg) were extracted with 10 mL of 90% acetone in the dark at 4 °C for 24 h. Following centrifugation, the absorbance of the supernatant was measured at 750, 664, 647, and 630 nm. Chlorophyll-a concentration was calculated using the equation proposed by Jeffrey and Humphrey (1975) and expressed as mg per gram of dry weight (mg/g DW) [24].

2.4. DNA Extraction and Sequencing

Genomic DNA was extracted from each sample using the ALFA-SEQ Advanced Soil DNA Kit (Guangzhou Magigene Biotechnology Co., Ltd., Guangzhou, China) according to the manufacturer's protocol. DNA was extracted individually from each of the three biological replicates per treatment (12 samples total). No technical replicates were performed for sequencing; each biological replicate was sequenced once. DNA concentration and purity were determined using a NanoDrop One spectrophotometer (Thermo Fisher Scientific, Waltham, MA, USA). For high-throughput sequencing, the V4/V5 hypervariable region of the 16S rRNA gene was amplified with barcoded primers 515F (5′-GTGCCAGCMGCCGCGGTAA-3′) and 907R (5′-CCGTCAATTCMTTTRAGTTT-3′), while the 18S rRNA gene was amplified using barcoded primers 547F (5′-CCAGCASCYGC GGTAATTCC-3′) and V4R (5′-ACTTTCGTTCTTGATYRA-3′) [25]. PCR amplification was performed with the extracted DNA as the template, and the amplicons were verified by 1% agarose gel electrophoresis. The PCR reaction system contained barcoded primers and Premix Taq (TaKaRa), with specific targeting of the aforementioned sequencing regions. The concentration of PCR products was quantified using GeneTools Analysis Software (Version 4.03.05.0, SynGene, Bangalore, India), and the volume of each sample was normalized for equal-mass pooling. The pooled PCR products were recovered from the gel using the E.Z.N.A.® Gel Extraction Kit (Omega Bio-tek, Norcross, GA, USA), and the target DNA fragments were eluted with TE buffer. Sequencing libraries were then constructed using the ALFA-SEQ DNA Library Prep Kit (FINDROP Bio-safety Technology (Guangzhou) Co., Ltd., Guangzhou, Guangdong, China), following the manufacturer's protocol. The fragment size distribution of the constructed libraries was assessed using a Qsep400 High-throughput Nucleic Acid and Protein Analyzer (Huzhou Heze Biotechnology Co., Ltd., Huzhou, China), and the library concentration was accurately quantified with a Qubit 4.0 fluorometer (Thermo Fisher Scientific, Waltham, MA, USA). High-throughput sequencing was conducted on an Illumina platform by Magigene Biotechnology Co., Ltd. (Guangzhou, China; http://cloud.magigene.com/).

Raw reads were demultiplexed and quality-filtered using Trimmomatic v0.39. Reads with average quality score < Q20 or length < 200 bp were discarded. Chimeric sequences were identified and removed using VSEARCH v2.15.0. High-quality reads were clustered into operational taxonomic units (OTUs) at 97% sequence similarity using UPARSE v11.0. Taxonomy was assigned using the RDP classifier (Ribosomal Database Project, Michigan State University, East Lansing, MI, USA) (confidence threshold 70%) against the SILVA 138.1 database for 16S rRNA and the PR2 v4.14 database for 18S rRNA. After read joining,

the average sequence length was approximately 420 bp for the 16S amplicon and 350 bp for the 18S amplicon. Rarefaction was performed to a minimum sequencing depth of 20,000 reads per sample for 16S and 15,000 reads per sample for 18S.

2.5. Data Analysis

Alpha diversity indices (Chao1 and Shannon) were calculated using the same platform (http://cloud.magigene.com/ (accessed on 10 November 2025)). β-diversity was assessed by non-metric multidimensional scaling (NMDS) based on Bray–Curtis dissimilarities, also generated by the Magigene cloud platform. Beta diversity was tested by PERMANOVA (adonis2, 999 permutations). All statistical analyses were performed using the three biological replicates per treatment as independent observations.

Predicted functional potentials of bacterial (16S rRNA) and eukaryotic (18S rRNA) communities were annotated using FAPROTAX and FUNGuild v1.2, respectively, on the BioinCloud platform (https://www.bioincloud.tech/ (accessed on 20 November 2025)). FAPROTAX and FUNGuild are annotation-based tools that map taxonomic identities to literature-curated functional categories. These predictions do not directly measure metabolic activities. For FAPROTAX, the database is limited to prokaryotes with well-characterized functions. For FUNGuild, many 18S rRNA OTUs (especially non-fungal eukaryotes) cannot be assigned to guilds, and the assignments for fungi are dependent on taxonomic resolution and database completeness [26,27]. FAPROTAX does not include MP degradation pathways; such predictions would require metagenomic data.

Statistical differences in biomass, chlorophyll-a content, alpha diversity indices (Chao1 and Shannon), and predicted functional categories (FAPROTAX, FUNGuild) among different treatments were analyzed using one-way analysis of variance (ANOVA) followed by Duncan's multiple range test (post hoc) in SPSS 27. Bar charts and stacked bar charts were generated using Origin 2022 software.

2.6. Network Analysis

Microbial co-occurrence networks were constructed to identify key taxonomic units and their topological roles in the PB community. The analysis was performed using combined bacterial (16S) and eukaryotic (18S) OTUs to capture cross-kingdom interactions, which are important in periphytic biofilms. Networks were based on SparCC correlations ($|r| > 0.6$, $p < 0.05$) using the WGCNA package in R (version 4.5.1) [28]. To improve network reliability, the operational taxonomic unit (OTU) table was filtered to retain only those OTUs present in more than 30% of all samples and with an average relative abundance more than 0.01% [29]. Network visualization was conducted using Gephi software (version 0.9.2). Subsequently, in the R program (version 4.5.1), the network nodes were classified into four subcategories (peripheral nodes, connectors, module hubs and network hubs) based on within-module connectivity (Zi) and among-module connectivity (Pi) to distinguish the functional importance of each node. The network hubs, module hubs, and connectors are generally identified as keystone module members [30]. Network inference with only three replicates per treatment is limited. Larger sample sizes are needed for robust network construction. Therefore, all network results presented here are exploratory and hypothesis-generating.

3. Results

3.1. Effects of MPs on PB Biomass and Chlorophyll-a of PBs

Variations in PB biomass and chlorophyll-a content under different MP addition treatments are presented in Figure 1. Compared with the CKU group, the biomass in the PAN, PE, and PET addition groups was significantly increased by 331.9%, 199.1%, and

173.7%, respectively. Concurrently, chlorophyll-a content in these MP-treated groups also increased significantly by 115.4%, 64.1%, and 48.5%, respectively.

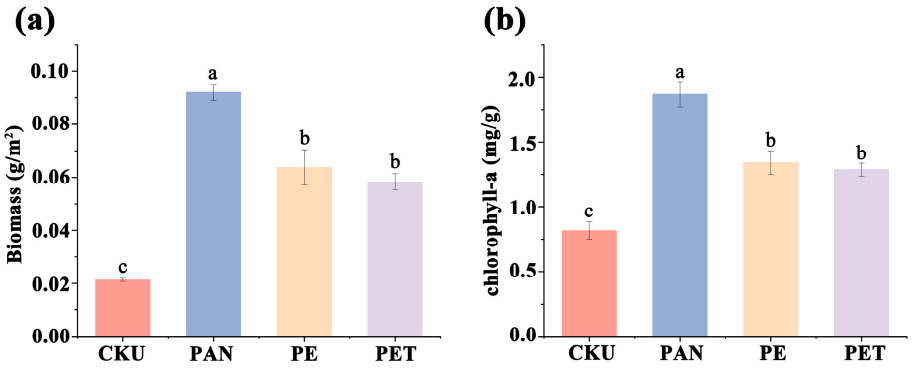


Figure 1. Comparison of the biomass (**a**) and chlorophyll-a (**b**) content of PBs added with different types of MPs. Different letters above error bar indicate significant differences between samples (n = 3) at $p < 0.05$ using ANOVA test. CKU: control group; PAN: polyacrylonitrile; PE: polyethylene; PET: polyethylene terephthalate.

3.2. Effects of MPs on PB Microbial Composition and Co-Occurrence Network

The α-diversity of microbial communities in different samples was evaluated using the Chao1 and Shannon indices. Non-metric multidimensional scaling (NMDS) was employed to assess β-diversity and illustrate community composition differences among treatments. Figure 2 showed that the differences in α-diversity among each group were not significant ($p > 0.05$). Compared with the CKU group, the α-diversity of bacteria in the soil decreased with the addition of MPs. For eukaryotic microbes, α-diversity was higher in the PE group than in the CKU group, whereas lower α-diversity was detected in the PAN and PET groups. It can be seen in Figure 2 that the bacterial community composition varies significantly among different groups, but the effect of MPs on the eukaryotic microbial community composition is not significant. β-diversity analysis revealed distinct responses of bacterial and eukaryotic communities in MP-treated groups. The bacterial community structure differed significantly among treatments (Figure 2c; stress = 0.092, p = 0.003, R^2 = 0.3911), whereas no significant structural differentiation was observed in eukaryotic communities (stress = 0.162, p = 0.101, R^2 = 0.3422).

The dominant bacterial phyla across all treatments included Cyanobacteria, Proteobacteria, Chloroflexi, Actinobacteriota, Bacteroidota, Firmicutes, and Acidobacteria (Figure 3a). The relative abundance of Chloroflexi and Actinobacteriota were lower in MP-treated groups. In all groups, the phyla Cyanobacteria and Proteobacteria were collectively dominant, accounting for 55% to 66% of the total abundance. At the genus level, four of the top 10 most abundant genera (*Phormidium_IAM_M-71*, *Dolichospermum_NIES41*, *Coleofasciculus_PCC-7420*, and *Pleurocapsa_PCC-7319*) belonged to Cyanobacteria (Figure 3c). Compared with the CKU group, the relative abundances of Bacteroidota and Proteobacteria increased under the MP treatment. The relative abundances of *A4b*, *Sphingomonas*, and *Saccharimonadales* showed little difference among all treatments. In every treatment, their relative abundances remained incredibly high. The relative abundance of the *Subgroup_22* decreased, while the relative abundances of *Pleurocapsa_PCC-7319*, *Phormidium_IAM_M-71*, *Dolichospermum_NIES41* and *Bacillus* all showed varying degrees of increase.

The β-diversity of eukaryotes showed no obvious structural differentiation. However, there were some differences among specific phyla and genera within different groups. Holozoa and Ascomycota were the dominant eukaryotic phyla across all groups, with a combined relative abundance ranging from 38.7% to 48.6% (Figure 3b). The relative abundance of *Ciliophora* was higher in the CKU and PAN groups than in the other two

groups, and its dominant genera (*Obertrumia* and *Bursaria*) showed the same variation trend. Compared with the CKU group, the relative abundance of Blastocladiomycota increased in the MP addition groups. The relative abundances of *Catenaria*, *Paraphysoderma* belonging to Blastocladiomycota, as well as *Dictyamoeba* and *Ischnamoeba* belonging to Incertae_Sedis, all increased (Figure 3d).

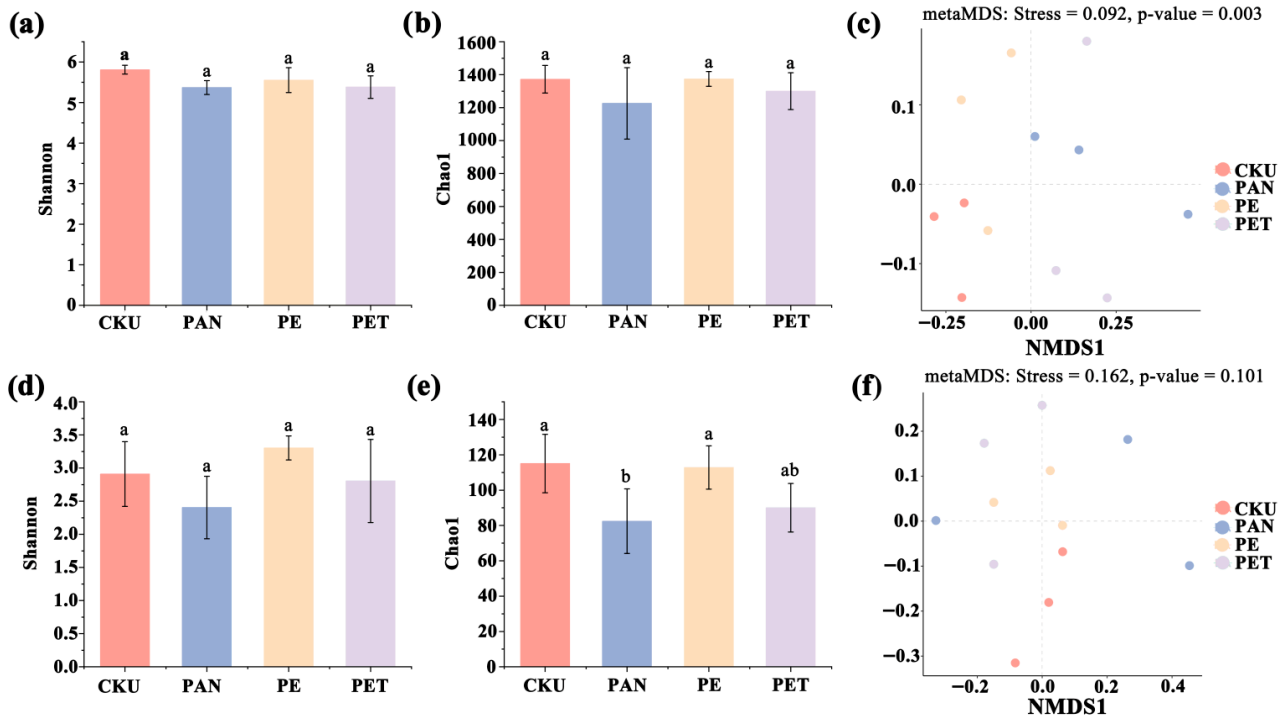


Figure 2. Differences in bacterial and eukaryotic community diversity under different treatments. Different letters above error bar indicate significant differences between samples ($n = 3$) at $p < 0.05$ using ANOVA test. α-Diversity index, Shannon (**a**) and Chao1 (**b**) index in bacterial community under different treatments. α-Diversity index, Shannon (**d**) and Chao1 (**e**) index in eukaryotic community under different treatments. β-Diversity index of bacterial (**c**) and eukaryotic (**f**) community. CKU: control group; PAN: polyacrylonitrile; PE: polyethylene; PET: polyethylene terephthalate.

Co-occurrence networks were constructed for each group to characterize microbial interactions and their responses to MP addition. These networks represent potential associations; they do not directly demonstrate ecological interactions or stability. The topological roles of individual taxa were further identified based on within-module connectivity (Zi) and among-module connectivity (Pi). Most nodes were classified as peripherals, with most links occurring within their own modules. The network in the PE group was the largest, with 1332 nodes and 2144 edges, and exhibited the highest average degree (3.219) and shortest path length (6.418) (Table 1). This group also showed the lowest modularity (0.63) and the highest proportion of negative correlations (0.4431). In comparison, the PAN group network possessed the highest modularity (0.718) and contained the only network hub.

Based on Zi-Pi analysis (Figure 4b), connectors were mainly affiliated with Proteobacteria and Chloroflexi. Module hubs were primarily composed of Cyanobacteria, Actinobacteriota, and Chloroflexi. The PE network exhibited the highest keystone taxon diversity, which was dominated by Chloroflexi and Proteobacteria. The PAN network was dominated by Proteobacteria and displayed a simpler structure.

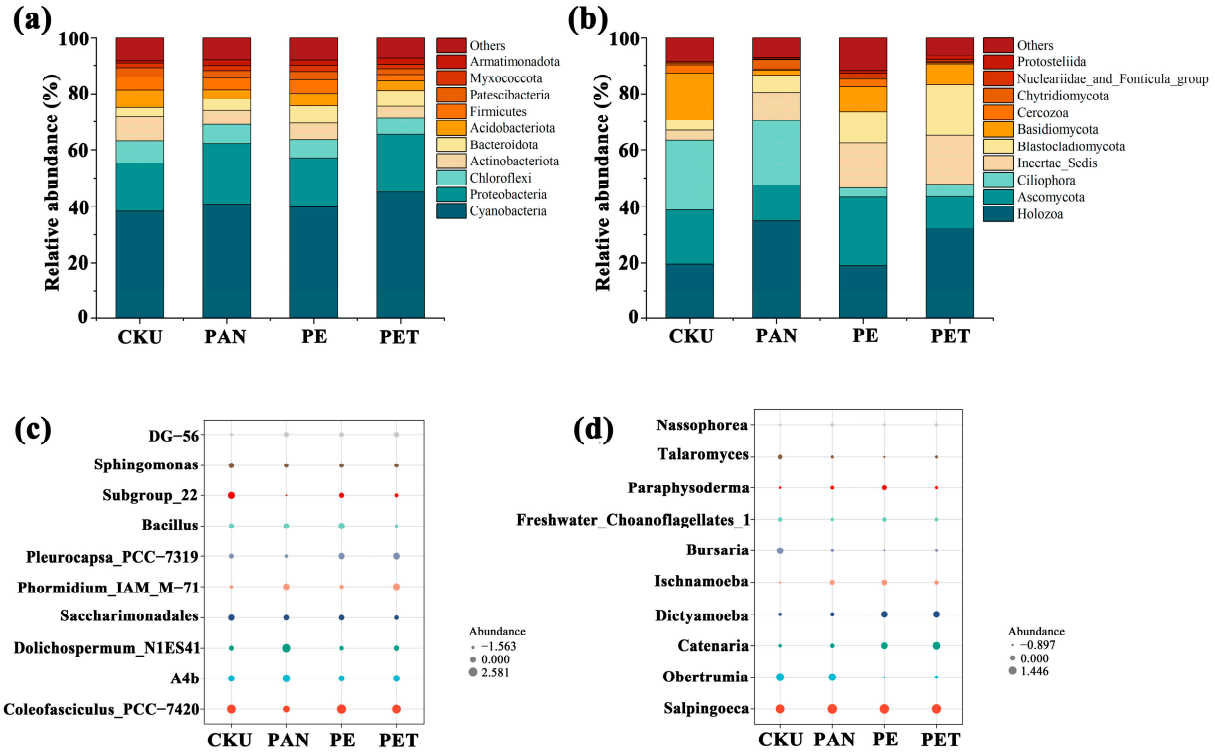


Figure 3. Differences in the composition and structure of bacterial and eukaryotic communities under different microplastic treatments. The composition of bacterial (**a**) and eukaryotic (**b**) phyla levels under different microplastic treatments. Relative abundances of the top ten dominant genera of bacteria (**c**) and eukaryotes (**d**) under different microplastic treatments. CKU: control group; PAN: polyacrylonitrile; PE: polyethylene; PET: polyethylene terephthalate.

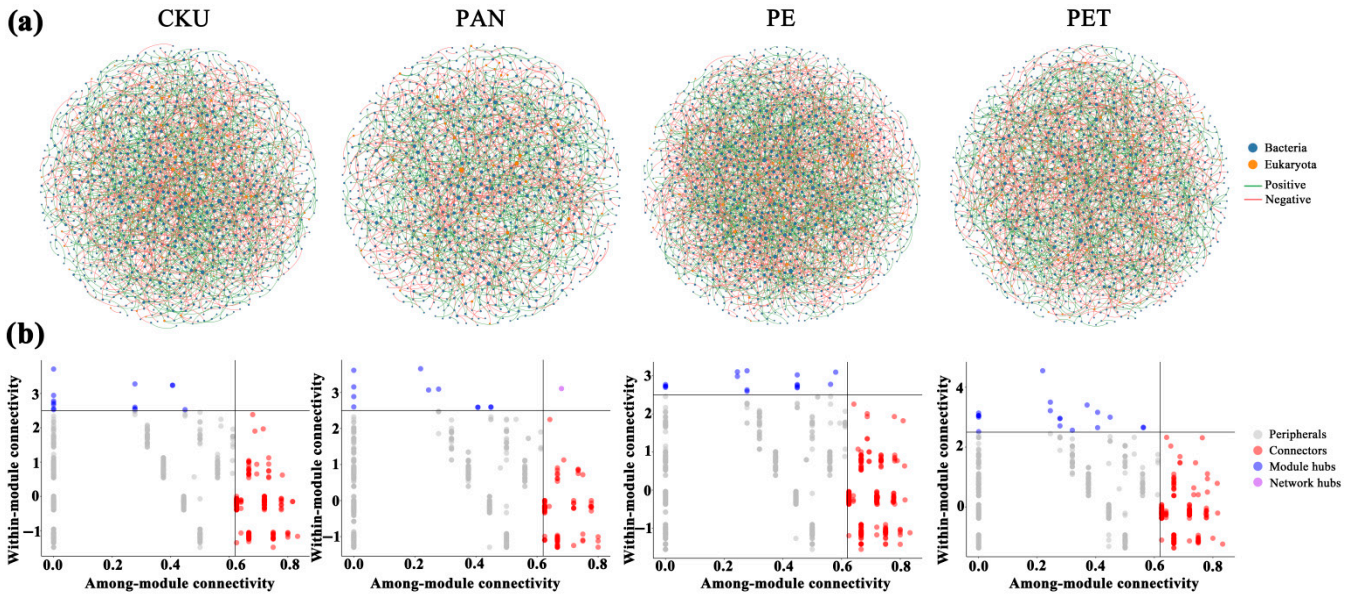


Figure 4. Co-occurrence patterns of the bacterial and eukaryotic community under different treatments. (**a**) Microbial co-occurrence networks under different treatments. A connection represents a strong ($|r| > 0.6$) and significant ($p < 0.05$) correlation between genera. The nodes are colored based at the kingdom level for microorganisms. (**b**) Roles of nodes in co-occurrence networks shown by the distribution of their within-module connectivity (Zi) and among-module connectivity (Pi). CKU: control group; PAN: polyacrylonitrile; PE: polyethylene; PET: polyethylene terephthalate.

Table 1. Topological parameters of microbial co-occurrence networks under different treatments.

Group	Modularity	Node	Edge	Average Degree	Average Clustering Coefficient	Average Path Length	Positive	Negative
CKU	0.677	1231	1841	2.991	0.018	6.972	58.83%	41.17%
PAN	0.718	1095	1543	2.818	0.02	7.303	57.81%	42.19%
PE	0.63	1332	2144	3.219	0.012	6.418	55.69%	44.31%
PET	0.663	1239	1890	3.051	0.017	6.784	56.61%	43.39%

CKU: control group; PAN: polyacrylonitrile; PE: polyethylene; PET: polyethylene terephthalate.

3.3. Effects of MPs on Predicted Function of PBs

Functional profiles of the PB bacterial community were predicted using FAPROTAX, and the results are presented in Figure 5a. Statistical comparisons (ANOVA and Duncan's test) were performed on the relative abundances of predicted functional categories. The results demonstrate that MPs significantly alter the microbial community's predicted functional potential. Among the predicted functional categories, photoautotrophy, chemoheterotrophy, and nitrate reduction maintained relatively high abundances across all treatments. Compared with the CKU group, nitrate reduction was significantly enhanced in the MP-treated groups, with the PE group showing the most prominent increase (approximately 135%). Similarly, denitrification activity was markedly elevated, and the PET group exhibited the highest potential, with an increase of approximately 280% relative to the CKU group. In contrast, the natural polymer degradation capacity was substantially suppressed in all MP-treated groups, with ligninolysis decreasing by approximately 92%. PE and PET groups showed approximately 150% higher plastic degradation potential compared to the CKU group. The CKU group maintained characteristic natural environment-driven functionality, demonstrating stronger nitrogen fixation capacity (approximately 75% higher than the PE group) and generally superior cellulose degradation capability compared to most MP-treated groups.

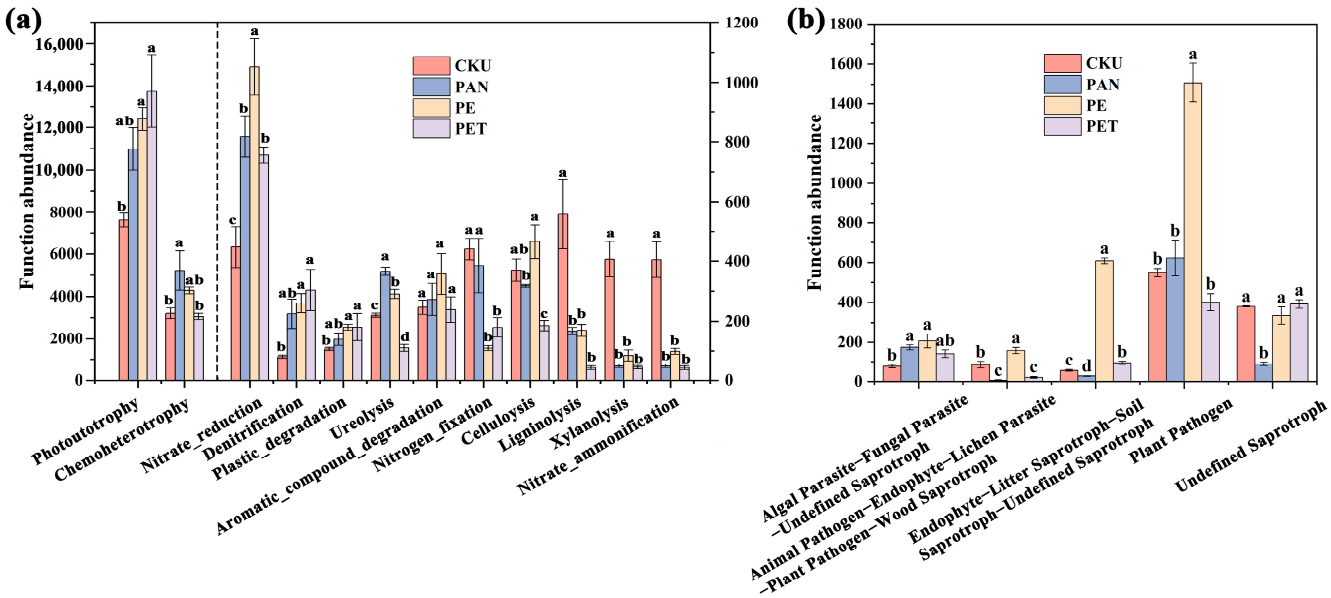


Figure 5. Functional annotations of bacteria (**a**) and eukaryotes (**b**) under different treatments. CKU: control group; PAN: polyacrylonitrile; PE: polyethylene; PET: polyethylene terephthalate. Different letters above error bar indicate significant differences between samples (n = 3) at $p < 0.05$ using ANOVA test.

Functional profiles of the PB eukaryotic community were predicted using FUNGuild, as shown in Figure 5b. The predicted functional potential of the eukaryotic community revealed type-specific impacts of MPs. The PE addition significantly increased plant pathogens ($p < 0.05$). In contrast, PAN and PET groups generally had lower relative abundances of these guilds compared to PE.

Across all MP addition groups, natural polymer degradation (cellulolysis, ligninolysis, xylanolysis, ureolysis) was suppressed, whereas plastic degradation potential was enhanced, especially in the PET group. Nitrogen cycling-related functions were significantly altered: nitrate reduction and denitrification were increased, while nitrogen fixation and nitrate ammonification were decreased. Eukaryotic functional shifts exhibited MP-type specificity: pathogenic fungi were suppressed in the PAN group but enriched in the PE group.

4. Discussion

4.1. The Effect of MPs on PB Growth

The significant increase in PB biomass and chlorophyll-a across MP treatments suggests that MPs may serve as new, advantageous substrates for biofilm colonization [19]. A combination of physicochemical and ecological mechanisms is probably responsible for the reported biomass enhancement, which exceeds 300% for PAN. MPs primarily provide additional firm surfaces for microbial attachment, which can be a limiting factor for PB growth in environments where natural hard substrates are scarce [19,31]. Polymer-specific surface chemistry likely acts as an initial selective filter. Hydrophilic PAN and PET promote different colonizers than hydrophobic PE [19,32]. Beyond serving as physical substrates, MPs become embedded within the three-dimensional EPS matrix of PBs. EPS secretion facilitates MP entrapment and creates stable microenvironments with altered oxygen and nutrient gradients. Such micro-scale anoxic sites favor facultative anaerobes (e.g., denitrifiers), consistent with our predicted functional shifts [33].

The concurrent rise in chlorophyll-a across all MP treatments indicates enhanced photosynthetic capacity of the PBs [14]. Notably, the magnitude of chlorophyll-a increase varied with polymer type, reflecting their distinct physicochemical properties. PAN addition resulted in the highest chlorophyll-a increase (115.4%), suggesting that the surface characteristics of PAN may particularly favor photosynthetic microorganisms. Previous studies have shown that PAN can significantly affect chlorophyll content in algae, typically causing inhibitory effects on chlorophyll-a and b synthesis [32]. PET also promoted chlorophyll-a synthesis in our study, consistent with findings that PET at certain concentrations can enhance algal chlorophyll production [34]. In contrast, PE showed a relatively moderate chlorophyll-a increase, which aligns with reports that PE can inhibit chlorophyll-a content in some aquatic plants [35]. These polymer-specific effects on chlorophyll-a likely result from differences in surface properties, leachable compounds, and their effect in the photosynthetic community structure within the biofilm. The increased photosynthetic capacity, fueled by enhanced light capture on MP surfaces and nutrient-rich microenvironments, ultimately supports the higher biomass observed across all MP treatments.

4.2. Responses of PB Community Structure to MPs

Bacterial and eukaryotic communities of PBs exhibited contrasting responses to MP addition. Bacterial communities showed significant shifts in β-diversity, indicating that different MP types act as environmental filters that select specific taxa adapted to the plastisphere niche [36]. Our finding that *Cyanobacteria* were enriched under PE treatment is consistent with previous research, which also observed a significant increase in *Cyanobacteria* abundance in periphytic biofilms exposed to polyethylene MPs [37]. The

consistent enrichment of *Cyanobacteria*, Proteobacteria and some biofilm-forming genera further supports the occurrence of trait-based selection under MP addition [38].

In contrast, eukaryotic community structure remained relatively stable across treatments, which may be attributed to higher inherent stability or stronger effects of stochastic processes [39]. This decoupling of bacterial and eukaryotic responses is ecologically important because cross-kingdom interactions are essential for maintaining PB function [40]. Despite the overall stability at the community level, MPs still induced some changes at finer taxonomic levels in both bacteria and eukaryotes. The observed shifts in certain genera, including parasitic fungi and ciliates, suggested altered host availability and grazing pressure [41].

Co-occurrence network analysis suggested that MP addition may reconfigure potential microbial interactions. Topological features differed descriptively between PE and PAN treatments. The network associated with PE was large and highly connected but exhibited low modularity and a high proportion of negative correlations. Similar topologies have been observed in communities under environmental stress [42,43]. The heterogeneous resource landscape formed by PE may enhance both interactions and competition, while the high diversity of keystone taxa could provide functional redundancy to buffer against disturbance [32,44]. In comparison, the PAN-associated network displayed the highest modularity and a clear hub structure. High modularity may help compartmentalize the network and limit the spread of disturbances, potentially contributing to community resilience [45].

MP addition shapes PB microbial communities by altering both taxonomic composition and interspecies interaction networks. Bacterial communities are more sensitive to MP addition and undergo obvious compositional filtering, whereas eukaryotic communities maintain overall structural stability with only subtle taxonomic adjustments. Different MP types drive divergent network architectures: PE may support a highly connected but competitively unstable network, while PAN may foster a modular, stable and specialized network structure. The responses of specific microbial taxa and the topological changes in co-occurrence networks collectively highlight the potential of PBs as a valuable biological indicator for assessing MP pollution in paddy ecosystems.

Due to the small sample size (n = 3 per treatment) and the large number of low-abundance taxa, we did not perform statistical tests on phylum- or genus-level relative abundances. Therefore, all taxonomic differences reported in this study are descriptive observations and should be interpreted with caution.

4.3. Predicted Functional Potential of PBs in Response to MPs

Functional prediction indicated that MP addition significantly altered the metabolic functions of PBs. The most prominent change was a metabolic shift in bacterial communities. Pathways involved in natural polymer degradation, including ligninolysis and cellulolysis, were significantly inhibited, whereas the potential for plastic degradation was enhanced [46]. Consistent with this shift, *Cyanobacteria* (enriched in MP treatments) perform photosynthesis and can express PET-degrading enzymes [47]. These results suggest that MPs exert selective pressure that redirects microbial metabolism from the decomposition of natural organic matter toward the breakdown of synthetic polymers [48,49].

Functional prediction also revealed substantial alterations in nitrogen metabolism following MP addition. Nitrate reduction and denitrification were enhanced, especially in the PE treatment. By contrast, nitrogen fixation and nitrate ammonification were inhibited across all MP-treated groups. *Proteobacteria* (enriched in PAN/PET) contain gene sets for denitrification and plastic degradation, whereas *Actinobacteriota* (decreased) are involved in natural polymer decomposition, aligning with suppressed ligninolysis [50]. Furthermore,

carbon leaching from polymer types may contribute to the observed biomass differences. PE is largely inert and provides limited bioavailable carbon, while PAN and PET may release low molecular weight compounds including monomers, oligomers, and additives that serve as supplemental carbon sources for heterotrophic bacteria [12,20].

Eukaryotic functional analysis based on FUNGuild further revealed type-specific ecological effects of MPs. The growth-promoting effect of PAN may be attributed to a dual mechanism. PE addition significantly enriched plant pathogens. This enrichment may be related to the hydrophobic surface and carbon supply provided by PE, which selectively favor pathogenic fungal taxa capable of colonizing synthetic substrates [12]. This aligns with evidence that MPs remodel fungal community composition and metabolic functions [51]. Such pathogen enrichment leads to an ecological trade-off, in which the productivity improvement driven by bacteria may be offset by elevated disease risks. These results highlight that shifts in eukaryotic functions are critical in mediating the ecological effects of MPs, and the overall impacts cannot be fully evaluated based only on bacterial indicators or biomass changes [42].

4.4. Limitation and Future Directions

Several limitations should be acknowledged. Functional predictions from 16S/18S rRNA data (FAPROTAX, FUNGuild) are annotation-based and do not measure actual metabolic activities; shotgun metagenomics or metatranscriptomics would be needed to directly detect plastic-degrading enzyme genes and their expression. Additionally, MPs persist in soils for years to decades, yet our experiment lasted only 30 days. Future studies should include lower, field-relevant concentrations; larger replicate numbers; direct functional assays (e.g., enzyme activities, qPCR, metagenomics); and long-term field or mesocosm experiments to validate our findings and assess profound effects.

5. Conclusions

This study demonstrates that the addition of MPs in soil significantly affects the growth, microbial community composition, and predicted functions of PBs in paddy ecosystems. Among the three types of MPs tested, PAN exerted the most pronounced effects on PB biomass accumulation and community structure. MPs act as environmental filters to reshape PB communities. The relative abundance of *Chloroflexi* and *Actinobacteriota* decreased in all MP treatments. *Cyanobacteria*, *Proteobacteria*, *Catenaria*, and *Obertrumia* showed descriptive responses to different MPs. These taxonomic shifts, along with the observed topological changes in microbial co-occurrence networks induced by MPs, suggest potential indicators for MP pollution. Compared with the PAN group, the PE and PET groups exhibited distinct impacts on microbial functional potentials related to polymer degradation and nitrogen metabolism. Overall, this is the first comparative assessment of PAN, PE, and PET effects on periphytic biofilms at the paddy soil–water interface, suggesting that PB community characteristics (e.g., *Cyanobacteria* abundance, network modularity) may serve as potential bioindicators for MP pollution in paddy fields.

Author Contributions: Conceptualization, H.L.; methodology, H.L.; validation, Y.D.; formal analysis, Y.D.; investigation, H.L., C.H., S.P., X.L., L.C. and Y.Z.; resources, H.L.; writing—original draft preparation, Y.D.; writing—review and editing, H.L., C.H., S.P., X.L., L.C. and Y.Z.; visualization, Y.D.; supervision, H.L. and Y.Z.; project administration, H.L.; funding acquisition, H.L. All authors have read and agreed to the published version of the manuscript.

Funding: This research and APC were funded by the National Natural Science Foundation of China [grant number 42277408].

Data Availability Statement: The data presented in this study are available on request from the corresponding author.

Conflicts of Interest: The authors declare no conflict of interest.

References

1. Geyer, R.; Jambeck, J.R.; Law, K.L. Production, use, and fate of all plastics ever made. *Sci. Adv.* **2017**, *3*, e1700782. [CrossRef]
2. Ye, Q.Y.; Wu, Y.X.; Liu, X.C.; Wu, J.Y.; Wu, P.X.; Wu, W.C. Microplastics abundance associated with farmland use types and the impact on soil microbial communities: A case study in Southern China. *J. Hazard. Mater.* **2024**, *480*, 136477. [CrossRef]
3. Rifhat, R.; Gao, P. Characterizing Microplastic Pollution and Microbial Community Status in Rice Paddy Soils Across Varied Environmental Settings in Songjiang, Shanghai. *Int. J. Innov. Sci. Res. Technol.* **2024**, *9*, 2850–2871. [CrossRef]
4. Huang, Y.; Liu, Q.; Jia, W.; Yan, C.; Wang, J. Agricultural plastic mulching as a source of microplastics in the terrestrial environment. *Environ. Pollut.* **2020**, *260*, 114096. [CrossRef]
5. Nizzetto, L.; Langaas, S.; Futter, M. Pollution: Do microplastics spill on to farm soils? *Nature* **2016**, *537*, 488. [CrossRef]
6. Rillig, M.C.; Lehmann, A. Microplastic in terrestrial ecosystems. *Science* **2020**, *368*, 1430–1431. [CrossRef]
7. Zhu, F.X.; Doyle, E.; Zhu, C.Y.; Zhou, D.M.; Gu, C.; Gao, J. Metagenomic analysis exploring microbial assemblages and functional genes potentially involved in di (2-ethylhexyl) phthalate degradation in soil. *Sci. Total Environ.* **2019**, *689*, 359–368. [CrossRef]
8. Bandara, T.; Franks, A.; Clark, G.; Tang, C. Fate of nano/microplastics and associated toxic pollutants in paddy ecosystems: Current knowledge and future perspectives. *Earth Crit. Zone* **2024**, *1*, 100013. [CrossRef]
9. Bian, J.L.; Peng, N.; Zhou, Z.; Yang, J.; Wang, X. A critical review of co-pollution of microplastics and heavy metals in agricultural soil environments. *Ecotoxicol. Environ. Saf.* **2024**, *286*, 117248. [CrossRef]
10. Fei, Y.F.; Huang, S.Y.; Zhang, H.B.; Tong, Y.Z.; Wen, D.S.; Xia, X.Y.; Wang, H.; Luo, Y.M.; Barceló, D. Response of soil enzyme activities and bacterial communities to the accumulation of microplastics in an acid cropped soil. *Sci. Total Environ.* **2020**, *707*, 135634. [CrossRef]
11. Huang, Y.; Zhao, Y.R.; Wang, J.; Zhang, M.J.; Jia, W.Q.; Qin, X. LDPE microplastic films alter microbial community composition and enzymatic activities in soil. *Environ. Pollut.* **2019**, *254*, 112983. [CrossRef]
12. Sun, Y.Z.; Duan, C.X.; Cao, N.; Ding, C.F.; Huang, Y.; Wang, J. Biodegradable and conventional microplastics exhibit distinct microbiome, functionality, and metabolome changes in soil. *J. Hazard. Mater.* **2022**, *424*, 127282. [CrossRef]
13. Battin, T.J.; Besemer, K.; Bengtsson, M.M.; Romani, A.M.; Packmann, A.I. The ecology and biogeochemistry of stream biofilms. *Nat. Rev. Microbiol.* **2016**, *14*, 251–263. [CrossRef]
14. Liu, J.; Wu, Y.; Wu, C.; Muylaert, K.; Vyverman, W.; Yu, H.Q.; Muñoz, R.; Rittmann, B. Advanced nutrient removal from surface water by a consortium of attached microalgae and bacteria: A review. *Bioresour. Technol.* **2019**, *241*, 1127–1137. [CrossRef]
15. Wu, Y.H.; Liu, J.Z.; Rene, E.R. Periphytic biofilms: A promising nutrient-removal technology in wastewater treatment. *Ecotoxicol. Environ. Saf.* **2020**, *205*, 111110.
16. Marella, T.K.; Saxena, A.; Tiwari, A.; Datta, A.; Dixit, S. Treating agricultural non-point source pollutants using periphyton biofilms and biomass volarization. *J. Environ. Manag.* **2022**, *301*, 113869. [CrossRef]
17. Sabater, S. Periphyton as a tool for ecological assessment and management in river ecosystems. *Limnetica* **2021**, *40*, 255–268.
18. Zettler, E.R.; Mincer, T.J.; Amaral-Zettler, L.A. Life in the "plastisphere": Microbial communities on plastic marine debris. *Environ. Sci. Technol.* **2013**, *47*, 7137–7146. [CrossRef]
19. Rummel, C.D.; Jahnke, A.; Gorokhova, E.; Kühnel, D.; Schmitt-Jansen, M. Impacts of biofilm formation on the fate and potential effects of microplastic in the aquatic environment. *Environ. Sci. Technol. Lett.* **2017**, *4*, 258–267. [CrossRef]
20. Rong, L.; Wang, Y.; Meidl, P.; Baqar, M.; Li, A.; Wang, L.; Sun, H. Insights into soil microbial assemblages and nitrogen cycling function responses to conventional and biodegradable microplastics. *J. Hazard. Mater.* **2025**, *491*, 137889. [CrossRef]
21. Lu, R.K. *Analytical Methods of Soil and Agro-Chemistry*; China Agricultural Science and Technology Press: Beijing, China, 2000.
22. Hu, X.J.; Gu, H.D.; Wang, Y.B.; Liu, J.J.; Yu, Z.H.; Li, Y.S.; Jin, J.; Liu, X.B.; Dai, Q.W.; Wang, G.H. Succession of soil bacterial communities and network patterns in response to conventional and biodegradable microplastics: A microcosmic study in Mollisol. *J. Hazard. Mater.* **2022**, *436*, 129218. [CrossRef]
23. Qi, R.M.; Jones, D.L.; Tang, Y.Y.; Gao, F.X.; Li, J.W.; Yan, C.R. Regulatory path for soil microbial communities depends on the type and dose of microplastics. *J. Hazard. Mater.* **2024**, *474*, 134702. [CrossRef] [PubMed]
24. Jeffery, S.W.; Humphrey, G.F. New spectrophotometric equation for determining chlorophyll a, b, c1 and c2. *Biochem. Physiol. Pflanz.* **1975**, *167*, 194–204.
25. Stoeck, T.; Bass, D.; Nebel, M.; Christen, R.; Jones, M.D.M.; Breiner, H.W.; Richards, T.A. Multiple marker parallel tag environmental DNA sequencing reveals a highly complex eukaryotic community in marine anoxic water. *Mol. Ecol.* **2010**, *19*, 21–31. [CrossRef]
26. Louca, S.; Parfrey, L.W.; Doebeli, M. Decoupling function and taxonomy in the global ocean microbiome. *Science* **2016**, *353*, 1272–1277. [CrossRef]

27. Nguyen, N.H.; Song, Z.; Bates, S.T.; Branco, S.; Tedersoo, L.; Menke, J.; Schilling, J.S.; Kennedy, P.G. FUNGuild: An open annotation tool for parsing fungal community datasets by ecological guild. *Fungal Ecol.* **2016**, *20*, 241–248. [CrossRef]
28. Langfelder, P.; Horvath, S. Fast R functions for robust correlations and hierarchical clustering. *J. Stat. Softw.* **2012**, *46*, 1–17. [CrossRef]
29. Shi, Y.; Delgado-Baquerizo, M.; Li, Y.T.; Yang, Y.F.; Zhu, Y.G.; Peñuelas, J.; Chu, H.Y. Abundance of kinless hubs within soil microbial networks are associated with high functional potential in agricultural ecosystems. *Environ. Int.* **2020**, *142*, 105869. [CrossRef] [PubMed]
30. She, Z.X.; Pan, X.; Wang, J.; Shao, R.; Wang, G.C.; Wang, S.P.; Yue, Z.B. Vertical environmental gradient drives prokaryotic microbial community assembly and species coexistence in a stratified acid mine drainage lake. *Water Res.* **2021**, *206*, 117739. [CrossRef]
31. Wang, F.Y.; Zhang, X.Q.; Zhang, S.Q.; Zhang, S.W.; Sun, Y.H. Interactions of microplastics and cadmium on plant growth and arbuscular mycorrhizal fungal communities in an agricultural soil. *Chemosphere* **2020**, *254*, 126791. [CrossRef]
32. Lin, W.; Su, F.; Lin, M.Z.; Jin, M.F.; Li, Y.H.; Ding, K.W.; Chen, Q.H.; Qian, Q.R.; Sun, X.L. Effect of microplastics PAN polymer and/or Cu^{2+} pollution on the growth of Chlorella pyrenoidosa. *Environ. Pollut.* **2020**, *265*, 114985. [CrossRef] [PubMed]
33. Karimi, B.; Maron, P.A.; Chemidlin-Prevost Boure, N.; Bernard, N.; Gilbert, D.; Ranjard, L. Microbial diversity and ecological networks as indicators of environmental quality. *Environ. Chem. Lett.* **2017**, *15*, 265–281. [CrossRef]
34. Wang, T.T.; Liu, H.C. Effects of PET and Gallic Acid on Growth, Photosynthesis, and Oxidative Stress of Microcystis aeruginosa. *Water Air Soil Poll.* **2024**, *235*, 158. [CrossRef]
35. Wu, Y.M.; Guo, P.Y.; Zhang, X.Y.; Zhang, Y.X.; Xie, S.T.; Deng, J. Effect of microplastics exposure on the photosynthesis system of freshwater algae. *J. Hazard. Mater.* **2019**, *374*, 219–227. [CrossRef] [PubMed]
36. Zhou, J.Z.; Ning, D.L. Stochastic community assembly: Does it matter in microbial ecology? *Microbiol. Mol. Biol. Rev.* **2017**, *81*, e00002-17. [CrossRef]
37. Li, W.; Luo, D.; Yan, N.; Miao, L.; Adyel, T.M.; Kong, M.; Hou, J. Effects of polyethylene microplastics with different particle sizes and concentrations on the community structure and function of periphytic biofilms. *J. Environ. Chem. Eng.* **2023**, *11*, 111287. [CrossRef]
38. Amaral-Zettler, L.A.; Zettler, E.R.; Mincer, T.J. Ecology of the plastisphere. *Nat. Rev. Microbiol.* **2020**, *18*, 139–151. [CrossRef]
39. Langenheder, S.; Székely, A.J. Species sorting and neutral processes are both important during the initial assembly of bacterial communities. *ISME J.* **2011**, *5*, 1086–1094. [CrossRef]
40. Sabater, S.; Timoner, X.; Borrego, C.; Acuña, V. Stream biofilm responses to flow intermittency: From cells to ecosystems. *Front. Environ. Sci.* **2016**, *4*, 14. [CrossRef]
41. Drury, B.; Rosi, E.J.; Ambrose, R.F. Periphyton as a bioindicator of environmental conditions in flowing waters. *Freshw. Biol.* **2021**, *66*, 1379–1395.
42. Hernandez, D.J.; David, A.S.; Menges, E.S.; Searcy, C.A.; Afkhami, M.E. Environmental stress destabilizes microbial networks. *ISME J.* **2021**, *15*, 1722–1734. [CrossRef] [PubMed]
43. Boots, B.; Russell, C.W.; Green, D.S. Effects of microplastics in soil ecosystems: Above and below ground. *Environ. Sci. Technol.* **2019**, *53*, 11496–11506. [CrossRef] [PubMed]
44. Wagg, C.; Schlaeppi, K.; Banerjee, S.; Kuramae, E.E.; van der Heijden, M.G.A. Fungal-bacterial diversity and microbiome complexity predict ecosystem functioning. *Nat. Commun.* **2019**, *10*, 4841. [CrossRef]
45. Deng, Y.; Jiang, Y.H.; Yang, Y.F.; He, Z.L.; Luo, F.; Zhou, J.Z. Molecular ecological network analyses. *BMC Bioinform.* **2012**, *13*, 113.
46. Seeley, M.E.; Song, B.; Passie, R.; Hale, R.C. Microplastics affect sedimentary microbial communities and nitrogen cycling. *Nat. Commun.* **2020**, *11*, 2372. [CrossRef]
47. Moog, D.; Schmitt, J.; Senger, J.; Zarzycki, J.; Rexer, K.H.; Linne, U.; Erb, T.; Maier, U.G. Using a marine microalga as a chassis for PET degradation. *Microb. Cell Fact.* **2019**, *18*, 171. [CrossRef]
48. Gewert, B.; Plassmann, M.M.; MacLeod, M. Pathways for degradation of plastic polymers floating in the marine environment. *Environ. Sci. Process. Impacts* **2015**, *17*, 1513–1521. [CrossRef]
49. Mohanan, N.; Montazer, Z.; Sharma, P.K.; Levin, D.B. Microbial and enzymatic degradation of synthetic plastics. *Front. Microbiol.* **2020**, *11*, 580709. [CrossRef]
50. Fortin, S.G.; Uhlig, K.; Hale, R.C.; Song, B. Microplastic biofilms as potential hotspots for plastic biodegradation and nitrogen cycling: A metagenomic perspective. *FEMS Microbiol. Ecol.* **2025**, *101*, fiaf035. [CrossRef]
51. Deng, Y.; Xiang, P.; Zhang, M.; Wang, S.Q.; Zhou, X.D.; Liu, J.C.; Li, Q.; He, G.Q. Synthetic microbiota for microplastic degradation modulates rhizosphere fungal diversity and metabolic function in highland barley. *Front. Microbiol.* **2025**, *16*, 1711544. [CrossRef] [PubMed]

Disclaimer/Publisher's Note: The statements, opinions and data contained in all publications are solely those of the individual author(s) and contributor(s) and not of MDPI and/or the editor(s). MDPI and/or the editor(s) disclaim responsibility for any injury to people or property resulting from any ideas, methods, instructions or products referred to in the content.